American Journal of Materials Science 2024, 14(3): 45-53
DOI: 10.5923/j.materials.20241403.01

Eco-Friendly Coatings Obtained by Silica from Rice Husk Waste and Hydrophobization with Bio-Based Materials

Liliane C. G.de S. Santos[1], Monique A. Cotrim[1], Marys L. B. Almeida[2], Eliane Ayres[1,*]

[1]Design Postgraduate Program (PPGD), State University of Minas Gerais, Belo Horizonte, Brazil
[2]Department of Civil Engineering, Federal University of Minas Gerais, Belo Horizonte, Brazil

Abstract This study proposes an eco-friendly approach for coating ceramic surfaces to enhance water resistance. Initially, black calcined rice husk was acid-leached and thermally treated to produce light gray ash. From this ash, high-purity silica particles were successfully synthesized using sodium silicate as the precursor. The surface area, determined via BET analysis, was approximately 120 m²/g. Stearic acid and hydrogenated castor oil were evaluated as sustainable hydrophobizers for silica coatings applied to porous ceramic substrates. When hydrogenated castor oil was used, the water contact angle reached 151°. Compared to uncoated substrates, the total color change (ΔE*) was consistently between 5 and 10, which is acceptable for applications not involving the preservation of architectural heritage. This research outlines a cost-effective strategy to convert agro-industrial waste into hydrophobic coatings, offering environmental benefits and contributing to advancements in sustainable construction materials.

Keywords Agro-industrial waste, Rice husk silica, Bio-based hydrophobizers, Hydrophobic coating

1. Introduction

The upsurge of waste production, driven by population rapid growth, significantly affects both, the environment and economy. Methods for converting these wastes into economically valuable materials can circumvent this trouble (Sarma and Paul, 2024). The population growth puts pressure on the construction industry to build increasingly buildings to meet the needs of current and future generations (Amarasinghe *et al*., 2024). Consequently, a huge amount of construction and demolition waste, including concrete and bricks, among others, is produced (Amarasinghe *et al*., 2024). In this regard, green building materials, partially made from wastes, play a crucial role in minimizing the environmental impact of construction (Iwuanyanwu *et al*., 2024). A large number of possibilities of recycling waste building materials have been reported. Guendouz and Boukhelkhal (2018) replaced cement with different contents of bricks waste powder in mortar composition. Brick waste proved to be suitable as a substitute for cement in the manufacture of common mortars. This diagnosis was due a large extent to improvements in the mechanical performance of the mortars for replacement rates up to 15%. In other studies, recycling floor tile waste and ceramic wastes, such as tile ceramic waste and ceramic sanitary ware, was utilized by partial replacement of natural aggregate in flowable sand concrete (Guendouz *et al*., 2021; Guendouz and Boukhelkhal, 2019). The use of 60% floor tile waste in this kind of partial replacement led to an increase of 48 and 24% in compressive and flexural strength at 28 days, respectively. Further, the use of 60% of ceramic tile waste or 50% of ceramic sanitary led to an increase of 100 and 51% in compressive strength at 28 days, respectively. The increase in flexural strength at 28 days of age was about 48% with 60% of both ceramic wastes. However, with increasing temperature the compressive strength of the modified concrete decreased, when compared to the reference concrete, after reaching its highest value at 200°C.

On the other hand, food agro-industrial by-products such as peels, seeds, stems, bagasse, kernels and husk are rejected as waste and have been considered as environmental pollutants (Gómez-García *et al*., 2021). Alternatively, the recycling of organic wastes in the field of civil engineering might be considered, as long as the obtained products are not subjected to stringent quality standards (Boukhelkhal *et al*., 2021). This was the case of the work, which replaced the fine aggregate (sand) in self-compacting mortar by olive core waste with a weight fraction of 10–50% (Boukhelkhal *et al*., 2021). It was observed a decrease in compressive strength of about 62, 63, 70 and 93% at 7 days for self-compacting mortar with 10, 20, 30, 40 and 50% of olive core waste respectively, compared to control self-compacted mortar.

* Corresponding author:
eliane.ayres.pu@gmail.com (Eliane Ayres)
Received: Dec. 3, 2024; Accepted: Dec. 19, 2024; Published: Dec. 21, 2024
Published online at http://journal.sapub.org/materials

It became 50, 52, 58, 69 and 72% at 28 days with waste contents of 10, 20, 30, 40 and 50%, respectively.

According to the authors, the decrease in compressive strength by adding olive core waste is mainly due to the decrease in bulk density of mixtures.

Results of other works showed that the use of spent coffee grounds waste, as partial replacement of natural sand in different dosages between 5 and 20%, reduced the mechanical strength of sand concrete mixes (Guendouz and Boukhelkhal, 2018; Guendouz *et al*., 2022). Nonetheless, the presence of spent coffee grounds caused a reduction in the values of thermal conductivity of the sand concrete (48%). With contents of 15% and 20%, the sand concretes can be regarded as insulating materials (λ<1 W/m °C). As reported by the authors, it is possible to produce thermally insulating eco-friendly concrete for various types of structural elements.

Rice husk (RH) is an agricultural waste, either in its raw form or in ash form (RHA), with potential to attain value-added products (Zou and Yang, 2019). When RH is burnt, it gives rise to 17-20% of RHA that is made up of 87-93% of silica (SiO_2) and other metallic oxide impurities (Abbas *et al*., 2024; Endale *et al*., 2022; Ugheoke and Mamat, 2012). Various metal ions and unburned carbon influence the purity and color of RHA (Chandrasekhar et al., 2005). Particularly, if there is a significant amount of K_2O in the husk, during the combustion it can dissociate to form elemental potassium. This causes surface melting, and the carbon gets entrapped in this melt without contact with air, hence hindering its oxidation. This phenomenon contributes to the formation of black particles (Chandrasekhar *et al*., 2006). For leaching out these impurities, acid treatment with HCl is the most effective (Ugheoke and Mamat, 2012). By controlling the burn of husks after removing metallic oxides, white or grey silica with high purity can be obtained (Chandrasekhar *et al*., 2006). At higher temperatures, amorphous silica is converted into undesirable crystalline silica (Islam *et al*., 2024). Crystalline silica has several disadvantages with limited industrial applications (Junaidi *et al*., 2017; Nzereogu *et al*., 2023; Carlsen and Saito, 2024). Crystallization can also be accelerated by the presence of K_2O in the raw RH (Zou and Yang, 2019). Thus, pre-treating the RH with acid is likewise useful to prevent silica ash crystallization.

RHA is considered as the cheapest source for silica gel, which can be extracted by the sol-gel method. In this route, silica is removed from RHA in the form of sodium silicate. The treatment with acid converts the silica into the rigid three-dimensional network of colloidal silica (Lima *et al*., 2011; Prasad and Pandey, 2012).

Silica (SiO_2) is widely used as a coating to improve the surface properties of materials such as glass, metal and ceramics (Yuan *et al*., 2024). As stated in the review by Cannio et al. (2024), antifouling coatings derived from pretreated silica-rich RHA can reduce the cumulative water uptake in the concrete materials. However, first RHA was modified using fluoroalkyl silane in order to enhance the hydrophobicity. In fact, silica is hydrophilic due the presence of silanol groups (Si–OH) on its surface. In order to impart hydrophobicity into the substrate surface, SiO_2 particles can be modified through functionalization process (Kumar *et al*., 2024) or by applying the hydrophobizer solution onto the substrate coated with SiO_2 particles (Wu *et al*., 2022). Li and Xu (2020) obtained silicon dioxide coatings modified by (3-aminopropyl)triethoxysilane (ATS). These materials were obtained by mixing tetraethylorthosilicate, ATS, and OH-terminal polydimethylsiloxane. The effectiveness of the coatings for stone protection was assessed by water uptake and contact angle, among others. Despite the surfaces achieved high repellency, most of formulations are either not environmentally friendly enough to support large-scale manufacturing or prohibitively expensive to scale up (Bayer, 2020). Therefore, low-cost feasible alternatives have been investigated. Nehan *et al*. (2023) prepared hydrophobic coatings by mixing silica from rice husk ash and polydimethylsiloxane in various ratios. The hydrophobic solutions were coated on glass slides using a brush. They demonstrated the potential use as an anti-water coating on eyeglasses. Castillo and Galarza-Acosta (2024) modified silica nanoparticles, obtained from rice husk, by coating them with stearic acid. For this, they used two different methods: by directly impregnating the nanoparticles with a stearic acid solution, or by dissolving the silica and then mixing it with stearic acid to induce nanoparticle formation in the presence of the acid. In this setting, the present paper aims to present results in the field of sustainable building materials. For this, silica gel derived from rice husk ash ($RH\text{-}SiO_2$) has been obtained and characterized. Following this, it was applied as coating onto a porous ceramic substrate. The efficacy of stearic acid and hydrogenated castor oil as hydrophobizers was analysed. Figure 1 presents a graphical diagram of the main stages followed.

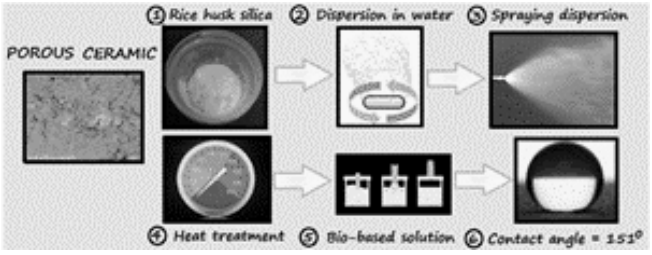

Figure 1. Graphical diagram with the main stages followed in the present study

2. Materials and Methods

2.1. Materials

Carbonized rice husk (CRH) was provided by Indiana Distribution (Embu das Artes, SP, Brazil). 1H,1H,2H,2H-perfluorodecyltriethoxysilane (PFDTES) (code: 658758) and fumed silica ($F\text{-}SiO_2$) (code: S5505) were purchased from Sigma-Aldrich (Merck KGaA, Darmstadt, Germany). Hydrogenated castor oil (HCO) was obtained from local

commerce (São Paulo, SP, Brazil) and stearic acid (STA) was from Synth (Diadema, SP, Brazil). The bisque ceramic tile (plain, unglazed, once-fired tile), with dimensions 15.3 × 15.3 × 0.3 cm, code SKU AZ0688, from Studio Flama (Belo Horizonte, MG, Brazil) was chosen as substrate. Other common laboratory reagents were used as received, with no purification treatment.

2.2. Production of Silica (RH-SiO_2) from CRH

The following procedure was adapted from other authors (Amutha *et al*., 2010; Moosa and Saddam, 2017). Firstly, 30g of the CRH was refluxed with 240 mL of HCl (6 M) for 3 h to leach metallic impurities. At the end of reaction, the acid was removed from the CRH by washing with distilled water several times in a vacuum filter using filter paper with a pore size of 0.45 μm. The acid treated CRH was then dried in an oven at 50°C for 6 h. Next, the dried CRH was subjected to thermal treatment at 650°C for 3 h to remove carbonaceous materials and gave rise to rice husk ash (RHA). The following step involved the preparation of sodium silicate. 25 g of treated RHA was stirred with 125 mL of hot water and 22 mL of 3 M sodium hydroxide. The solution was heated at 90°C for 2 h under magnetic stirring and vacuum filtered. The filtrate was the transparent, colorless sodium silicate solution. In the end, the sodium silicate solution was titrated with concentrated sulfuric acid to obtain a gel at pH 8.0. The gel was washed with distilled water until the pH was equal to 7.0 and then dried in an oven at 50°C for 48 h to form white silica powder.

2.3. Coating of RH-SiO_2 onto Porous Ceramic Substrate

Biscuit ceramic tile was used as a porous substrate to apply the coating. The biscuit ceramic tile (or bisque ceramic tile) refers to the tile that underwent the first firing, but it was not glazed. Firstly, biscuit ceramic tile was cut into small pieces (2 cm x 2 cm). The pieces were abundantly washed with ethanol and dried in an oven at 200°C. Then, 0.3 g of RH-SiO_2 was dispersed under ultrasonic agitation in 35 mL of deionized water. The dispersion was sprayed onto the surface of samples for 1 min using an airbrush at 15 cm. After drying at room temperature, the coated samples were thermally treated in an oven at 550°C for 1 h and cooled naturally (Wen *et al*., 2017). As a control, commercial fumed silica (F-SiO_2) was used instead of RH-SiO_2. In some samples, a solution of expanded polystyrene (EPS) in limonene (40% w/v) was brushing onto the surface of biscuit tile before spraying the silica dispersion. The polymeric film formed after drying acted as a sacrificial layer, which is removed during the thermal treatment (Lejnieks *et al*., 2010).

2.4. Surface Hydrophobization

After the thermal treatment, the coated biscuit tile was dipped for 1 min into the hydrophobizer solution, and then dried naturally in air. The solutions stearic acid (STA)/ethanol (2% w/v) and hydrogenated castor oil (HCO)/ethanol (2% w/v) were tested. 1H,1H,2H,2H-perfluorodecyltriethoxysilane (PFDTES) in hexane (1% w/v) was used as a control hydrophobizer (Wen *et al*., 2017).

2.5. Characterization

2.5.1. Fourier Transform Infrared (FTIR) Spectroscopy

The Fourier infrared spectrometer (Nicolet, model iS50 FT- IR- Thermo Scientific) in the range of 4000 cm^{-1} to 650 cm^{-1} was used to detect the typical sodium silicate and silica bands. Spectra were obtained with an average of 64 scans and a resolution of 2 cm^{-1}, using the Attenuated Total Reflectance (ATR) technique, with diamond crystal.

2.5.2. Specific Surface Area of RH-SiO_2 by BET Method

Brunauer-Emmett-Teller (BET) specific surface area analysis (Bardestani *et al*., 2019) was performed using 'Quantachrome, model NovaWin2' equipment (Anton Paar GmbH, USA). The sample was analyzed under a nitrogen atmosphere (adsorption-desorption isotherms at 77 K), using multipoint measurement, with relative pressures (P/P_0) ranging from 0.01 to 0.99.

2.5.3. X-Ray Diffraction (XRD)

XRD pattern of RH-SiO_2 was obtained using an X-ray diffractometer (PANalyticalX'Pert, Empyrean, Netherlands) operating at 40 kV/40 mA and equipped with a Cu tube (Cu Kα radiation, = 1.5406 Å) and a graphite crystal monochromator. Scanning was performed at 0.06° s^{-1} for 2θ = 3–90°. The crystallite average size was estimated using Equation 1, called the Debye–Scherrer diffraction equation (Moosa and Saddam, 2017).

$$D(2\theta) = \frac{K\lambda}{\beta \cos \theta} \quad (1)$$

Where: D is the average size of crystallite (nm); β is the width at half maximum of the peak in radians; θ is the Bragg angle (in radians); K is a dimensionless factor relating to the crystallite shape, generally considered as 0.9, and λ is the wavelength of X-Ray (Cu-Kα= 0.1541 nm).

2.5.4. Scanning Electron Microscopy (SEM)

The surface morphologies were observed with a bench model Hitachi 4000 Plus with an electron beam operating at 5 kV. The images were captured using the backscattered electron detector (BSD).

2.5.5. Contact Angle Measurement (CA)

The wettability of the coated ceramic substrate was assessed through the values of the contact angle (CA). The measurements were performed by the sessile drop method, with the aid of a DIGIDROP-DI goniometer (GBX Instruments). The results represent the average values of the total (right and left) contact angle with water (10 μL) for individual surface treatment methods. Contact angle values were calculated as mean values of three consecutive recordings, at room temperature, using the Surface Energy mode of the software.

2.5.6. Total Color Change (ΔE*)

The color change (ΔE*), considering the uncoated substrate as the reference, was analyzed using a Konica Minolta CM-600D spectrophotometer. The following operating conditions were used: SCE reflectance, scanning from 360 to 740 nm, and observer angle of 10° with D65 illuminant. The data were collected with the Spectra Magic NX software. Every coated sample was measured in three random points, and the color data represented the average of three measurements.

3. Results and Discussion

3.1. Process of Preparing Silica from Rice Husk Ash (RHA) and Characterization

When rice husk (RH) is calcined, two kinds of materials can produce depending on whether combustion is complete or incomplete. They are rice husk ash (gray or white RHA) and carbonized rice husk (black CRH), respectively (Ugheoke and Mamat, 2012). Herein, black CRH (Figure 2a) was acid treated with HCl, and then to a thermal treatment (650°C) to obtain a light gray ash (RHA) (Figure 2b).

The reaction of RHA with sodium hydroxide produces a sodium silicate solution. This solution is the filtrate after vacuum filtration at the end of the reaction. The titration with sulfuric acid generated a gelatinous precipitate, known as silica gel (Samy *et al.*, 2023). Silica gel is a type of amorphous SiO_2 that has a very porous structure (Gomes *et al.*, 2018). The RH-SiO_2 was obtained after drying and grinding the gel. The silica purity is controlled, among other parameters, by the concentration of NaOH (Yuvakkumar *et al.*, 2014).

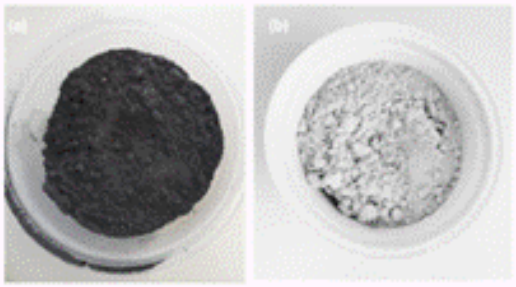

Figure 2. Photos of CRH as received (a) and RHA after CRH treated with HCl and thermal treatment at 650°C (b)

Equations 2 and 3 represent the subsequent reactions occurring in the process of obtaining the high-purity silica (Samy *et al.*, 2023).

$$SiO_2\,(RHA) + 2\,NaOH \longrightarrow Na_2SiO_3\,(\text{sodium silicate}) + H_2O \quad (2)$$

$$Na_2SiO_3 + H_2SO_4 \rightarrow SiO_2\,(RH - SiO_2) + Na_2SO_4 + H_2O \quad (3)$$

Figure 3 shows the FTIR spectra corresponding to the intermediary sodium silicate and the final product (RH-SiO_2).

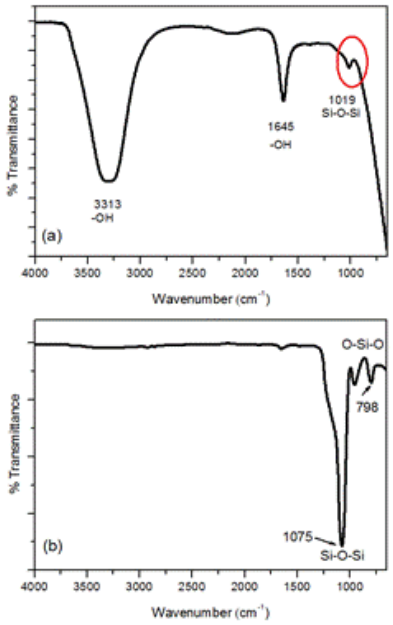

Figure 3. FTIR spectra of (a) sodium silicate and (b) RH-SiO_2 particles

Due to the strong absorption of water, the O-H stretching and O-H bending bands at 3313 cm^{-1} and 1640 cm^{-1}, respectively, stand out in the FTIR spectrum of sodium silicate (Figure 2a) (Zulfiqar *et al.*, 2016). Despite this, it is possible to notice the band at 1019 cm^{-1} due to the asymmetric stretching of Si-O-Si bonds (ν_{as}Si-O-Si) (Zulfiqar *et al.*, 2016; Vidal *et al.*, 2016).

Silica gel is a kind of amorphous silica that arises from the ionic exchange of Na^+ with H^+, followed by the lowering pH of sodium silicate solution. The product is a three-dimensional network of silica polymer that embodies the liquid phase (Matinfar and Nychka, 2023). Removal of water from the polymeric silica network, a phenomenon called syneresis, gives rise to the RH-SiO_2, which the FTIR spectrum is shown in Figure 2b.

In their review article, Matinfar and Nychka (2023) have explained that the intensity ratio $_{vas}$Si–O–Si/$_{\delta}$O-H continues to increase after gelation, suggesting the release of water along with the formation of Si-O-Si bonds during syneresis. The other band highlighted in the spectrum at 798 cm^{-1} is related to the symmetric Si–O–Si stretching (Yuvakkumar *et al.*, 2014). The absence of noticeable peaks at the 1281–2428 cm^{-1} range, attributed to impurities such as carbonate and sodium groups, suggests pure silica powder (Yuvakkumar *et al.*, 2014).

The BET surface area of the RH-SiO_2 is 122 $m^2\,g^{-1}$, which is much higher compared with that of RHA (5.5 $m^2\,g^{-1}$). Azat *et al.* (2019) demonstrated that the variability of raw RH leads to pure silica with a wide range of surface areas. In their work, the values varied from 112 $m^2\,g^{-1}$ to 980 $m^2\,g^{-1}$. Liou and Yang (2011) obtained nanosilica from rice husk ash (RHA) using the sodium silicate route followed by acid precipitation. Different acids were tested in the precipitation step. The surface area reached a maximum of 350 $m^2\,g^{-1}$ when hydrochloric acid (HCl) was used. The precipitation with

sulfuric acid (H_2SO_4) produced silica with a surface area of 320 m^2 g^{-1}. The authors have attributed the difference in surface areas to residual metals embedded in the gel matrix that block the pores. As reported by them, silica precipitated with HCl has higher surface area due to the lower sodium content. Since sodium chloride (NaCl) has minor size, it is easily removed by water washing.

The XRD pattern RH-SiO_2 particles (Figure 4) presents a broad peak at 23° (2θ), which confirmed the predominant amorphous nature of RH-SiO_2 (Moosa and Saddam, 2017; Jyoti *et al*., 2021).

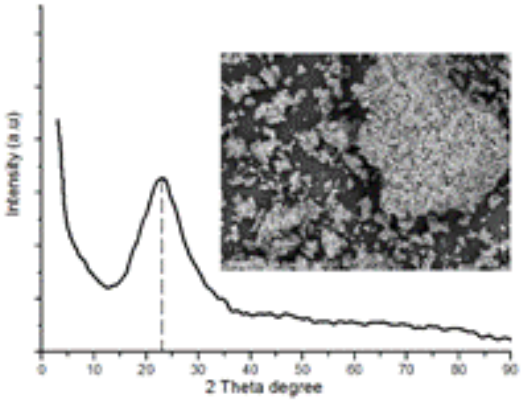

Figure 4. XRD pattern of RH-SiO_2. In detail the SEM image of RH-SiO_2

The amorphous character of silica was already expected. The carbonized rice husk (black CRH), used to produce RHA (ash), was submitted to acid leaching before the thermal treatment at 650°C. Under these conditions, silica crystallization does not occur, even at temperatures in the range of 800°C (Islam *et al*., 2024; Ajeel *et al*., 2021). Other authors reported the same result using a similar process to produce nanosilica derived from rice husk ash (Ajeel *et al*., 2021, Nayak and Datta, 2021). Despite the predominant amorphous character of RH-SiO_2, herein we have estimated the crystallite size by using the Scherrer equation (Eq. 1). The Scherrer method confirmed the amorphous character of RH-SiO_2, since the crystallite size was found to be around 1.0 nm. The crystallite size as small as 1.0 nm means that the amorphous regions are predominant in silica (Moosa and Saddam, 2017). Azhakesan *et al*. (2020) reported larger crystallites using the same method. They found 22 nm when RHA was produced from pyrolysis at 700°C or 800°C, and 5.0 nm at 750°C. Additionally, the SEM image of RH-SiO_2 (detail of Fig. 4) shows agglomeration of porous particles with irregular morphology, as previously reported (Ayswarya *et al*., 2021).

3.2. Coating and Hydrophobization

The biscuit ceramic tile although fired, it is not glassy, remains porous, and can absorb water. In some samples, a solution of expanded polystyrene (EPS) in limonene (sacrificial layer) was applied to avoid silica particles penetrate into the substrate pores. Table 1 presents the water contact angle values measured for the different coatings.

Table 1. Contact angle (CA) without and with polymeric sacrificial layer (PSL)

Silica	Hydrophobizer	CA	CA/PSL
F-SiO_2 (control)	**PFDTS**	**136°**	
RH-SiO_2	PFDTS	161°	
F-SiO_2	STA	123°	127°
RH-SiO_2	STA	125°	126°
F-SiO_2	HCO	103°	136°
RH-SiO_2	HCO	133°	151°

PFDTS= 1H, 1H, 2H, 2H-perfluorodecyltriethoxysilane; STA= stearic acid; HCO= Hydrogenated castor oil; F-SiO_2= commercial fumed silica and RH-SiO_2= silica from rice husk ash.

Based on the conventional wettability criteria, surfaces with static CA lesser than 90° are regarded as hydrophilic, whereas those with CA greater than 90° are hydrophobic (Kung *et al*., 2019). It is possible to notice the better water-repelling of RH-SiO_2 compared with F-SiO_2. This might be due to the higher surface area of F-SiO_2 (395 m^2 g^{-1}, according to the manufacturer), compared with RH-SiO_2 (122 m^2 g^{-1}). Fernandes *et al*. (2018) related higher water absorption to higher surface area in composites made from epoxy resin and RHA. Jembere and Fanta (2017) replaced commercial silica with silica derived from RHA as filler for natural rubber. As in the present work, they found surface area of RHA silica lower than that of commercial silica.

Figure 5 shows SEM images of coated ceramic substrate with RH-SiO_2 (Figure 5a) and F-SiO_2 (Figure 5b) before hydrophobization. It is easy to perceive the better dispersion of RH- SiO_2, which might also have contributed to the higher contact angle.

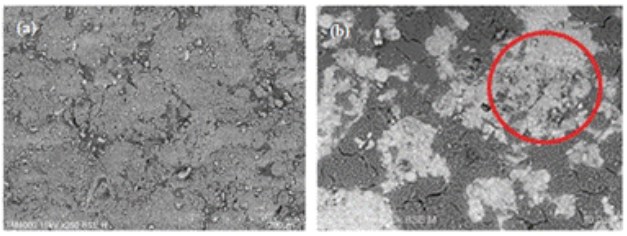

Figure 5. SEM images of ceramic substrate coated with (a) RH-SiO_2 and (b) F-SiO_2

On the other hand, replacing the fluorinated hydrophobizer is more challenging.

One example was given by Sauthier *et al*. (2014), who coated mica with stearic acid. They explained that many defects on the surface let water molecules penetrate into the layer, thus reducing its hydrophobic character. As a result, hydrophobicity was reached only with a thicker multilayer film.

In the present work, the presence of a polymeric sacrificial layer (PSL) was the strategy employed to minimize surface defects. The idea is that PSL provides a smooth substrate surface before it degrades during the thermal treatment to produce the coating (550°C). Figure 6 shows the SEM images of substrate surface uncoated (Figure 6a) and coated with PSL (Figure 6b).

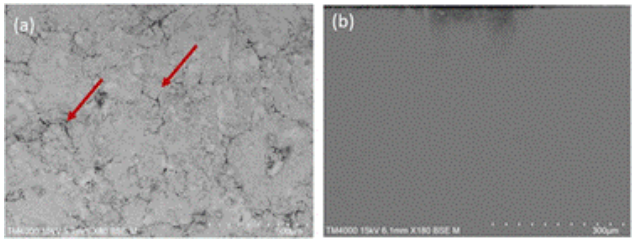

Figure 6. SEM images of the ceramic substrate: (a) uncoated and (b) coated with polymeric sacrificial layer (PSL)

As can be noted, the porosity disappeared when the surface is coated with PSL, enabling spraying the silica dispersion homogeneously (Figure 7). An increase in contact angle was detected for all samples previously coated with PSL (Tab. 1).

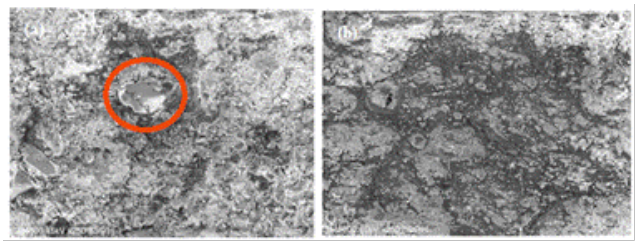

Figure 7. SEM images of ceramic substrate coated with RH-SiO_2 and hydrophobized with STA: (a) without PSL and (b) previously coated with PSL

Cho *et al*. (2021) have already reported the strategy of using a sacrificial layer. In their study, a graphene oxide interlayer (GO) allowed the porous ceramic substrate to be coated with a defect-free thin alumina nanoparticles layer. Before be removed during the calcination, the GO sacrificial layer prevented the pore clogging of the substrate by the alumina nanoparticles and gave rise to a uniform alumina layer.

Figure 8 shows SEM images of ceramic substrate coated with RH-SiO_2 and hydrophobized with hydrogenated castor oil (HCO). The growth of HCO spherulites on the surface masked the effect of sacrificial layer (Nakano *et al*., 2016). Therefore, there is no noticeable visual difference between the two micrographs. Bai *et al*. (2018) prepared various sustainable superhydrophobic coatings made of hydrogenated castor oil spherulites. As stated by them, the as-prepared coatings are suitable to various substrates, including paper or plastic filters and porous materials.

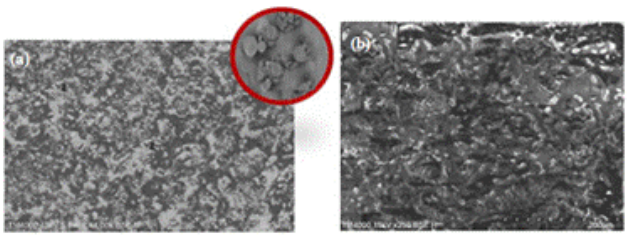

Figure 8. SEM images of ceramic substrate coated with RH-SiO_2 and hydrophobized with HCO: (a) without PSL and (b) previously coated with PSL

In the present work, the good performance of HCO as hydrophobizer was ascribed to the additional roughness on the substrate surface created by the spherulites.

3.3. Optical Appearance of Coated Ceramic Substrate: Total Color Change (ΔE*)

The effect of RH-SiO_2 coating on optical appearance of the substrate was performed using the total color change (ΔE*) given by Equation 2. The CIELab color space defines a color through three coordinates, L* (brightness: 0= black, 100= white), a*(+ red, - green), and b* (+ yellow, - blue) (Varışli *et al*., 2023).

$$\Delta E^* = \sqrt{(L - L_0)^2 + (a - a_0)^2 + (b - b_0)^2} \qquad (4)$$

Where: L-L_o is the difference in brightness between treated and untreated substrate, respectively; a-a_o is the difference in redness between treated and untreated substrate, respectively; b-b_o is the difference in yellowness between treated and untreated substrate, respectively.

Coatings must cause the minimum change in the aesthetic appearance of the substrate. Coatings are acceptable if the total color change of the substrate ΔE*<5 or even ΔE*<10, in cases that do not involve the preservation of architectural heritage. If ΔE*<1 the variation is not perceived by the human eye (Varışli *et al*., 2023). Adamopoulos *et al*. (2021) measured the ΔE* of substrates due to the deposition of silica sol solution used as protective coating. The results showed that the coating caused a negligible color change on the marble (ΔE*<3). The coating had practically no effect on the aesthetic appearance of paper (ΔE*=0.5). However, the coating had considerable and visible effects on the colors of silk (ΔE*=9.70) and wood (ΔE*= 12.80), and major effect on the appearance of brass (ΔE*=33.22) and Si wafers (ΔE*=56.72). Figure 9 shows the results of ΔE* of ceramic substrate with different coatings.

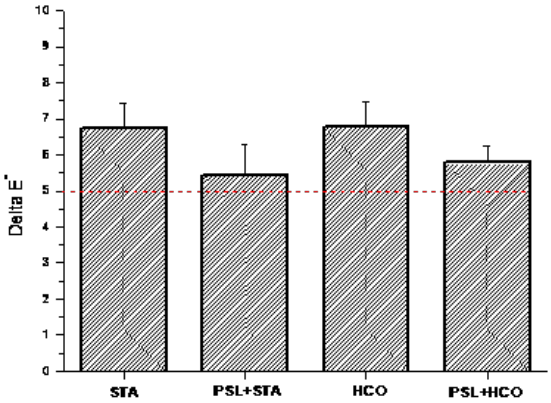

Figure 9. Total color change (ΔE*) of ceramic substrate coated with RH-SiO_2, in reference to uncoated substrate (standard). STA= stearic acid, HCO= hydrogenated castor oil, and PSL= polymeric sacrificial layer

As can be observed all samples presented values of 5.0< ΔE*<10, being PSL+STA with the minor ΔE*. The lower value of ΔE* when PSL is applied before coating might be attributed to the smoother surface of the substrate. Further, samples using HCO have a higher value of ΔE* compared with samples using STA. This is probably due to additional roughness imparted by the spherulites.

In the conventional cycle, the biscuit ceramic tile is glazed and fired at higher temperatures, around 1300 °C, to achieve

full resistance. This final firing requires about 50% of the total energy required in the entire process (Santos *et al*., 2020). As an alternative, Danu (2008) coated unglazed biscuit ceramic tile with UV-curing of titanium dioxide pigmented epoxy acrylate. According to him, UV-curing is more applicable for flat objects due to limiting of radiation exposure geometry. The author stated further that UV-cured coating provides lower coating properties than those of glazed ceramics. Nevertheless, coating technology presents advantage, for example, on environment point of view.

Surface modified biscuit ceramic tile might have potential for using on walls with a rustic aspect (Figure 10). In this case, the drawings on the surface were made with a pottery-carving tool before the substrate treatment.

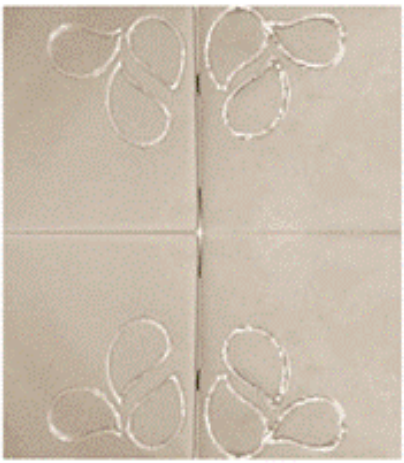

Figure 10. Photo of a wall panel made from coated (STA) biscuit ceramic tiles

As a reminder, biscuit ceramic tiles treated in this way are suitable for use on walls, but not for use on floors.

4. Conclusions

This research demonstrated the feasibility of transforming agro-industrial waste into hydrophobic coatings. Silica derived from rice husks was obtained using the sol-gel method, producing high-purity silica from a sodium silicate solution. This silica, dispersed in water, was applied to a porous ceramic substrate, and the coated samples underwent heat treatment. After consolidation of the particles, surface hydrophobization was performed using stearic acid (STA) or hydrogenated castor oil (HCO) as alternatives to fluorinated derivatives.

The study highlighted significant results, such as the replacement of environmentally harmful materials with sustainable alternatives. In addition, the use of a polymeric sacrificial layer (PSL) resulted in homogeneous silica coatings and improved contact angles. The roughness conferred by the HCO spherulites further increased water repellency. However, substrates hydrophobized with HCO exhibited higher total color change (ΔE*) values compared to those treated with STA, likely due to the additional surface roughness created by the spherulites.

This work highlights the potential of agro-industrial waste to contribute to sustainable construction. The authors hope to inspire continued research and development in waste-derived materials to explore innovative solutions of building materials. Mainly encouraging interdisciplinary collaboration among engineers, chemists, and designers.

ACKNOWLEDGEMENTS

This work was supported by the Minas Gerais State Research Support Foundation (FAPEMIG), the Coordination for the Improvement of Higher Education Personnel (CAPES) and the National Council for Scientific and Technological Development (CNPq).

REFERENCES

[1] Abbas, M. A., Kwan, W. H., Samsudin, M. H., Hai, T. K., 2024, Optimising Factors for the Production of Amorphous Rice Husk Ash via Combustion Process for Sustainable Construction: A Review. J. Adv. Res. Appl. Mech., 120(1), 50-61.

[2] Adamopoulos, F. G., Vouvoudi, E. C., Pavlidou, E., Achilias, D. S., Karapanagiotis, I., 2021, TEOS-based superhydrophobic coating for the protection of stone-built cultural heritage. Coatings, 11(2), 135.

[3] Ajeel, S. A., Sukkar, K. A., Zedin, N. K., 2021, The chemical extraction process for producing high-purity nanosilica from Iraqi rice husk. Eng. Techn. J., 39(1A), 56-63.

[4] Amarasinghe, I., Hong, Y., Stewart, R. A., 2024, Development of a material circularity evaluation framework for building construction projects. J. Clean. Prod., 436, 140562.

[5] Amutha, K., Ravibaskar, R., Sivakumar, G., 2010, Extraction, Synthesis, and Characterization of Nanosilica from Rice Husk Ash. Int. J. Nanotechnol. Appl., 4(1), 61-66.

[6] Ayswarya, E. P., Nair, A. B., Thachil, E. T., 2021, A comparative study of mechanical, dynamic mechanical and thermal properties of rice husk ash, modified rice husk ash and nanosilica-filled epoxy composites. Mater. Today Proc., 47, 5351-5357.

[7] Azat, S., Korobeinyk, A. V., Moustakas, K., Inglezakis, V. J., 2019, Sustainable production of pure silica from rice husk waste in Kazakhstan. J. Clean Prod., 217, 352-359.

[8] Azhakesan, A., Yadav, S., Rajesh, V. M., 2020, Extraction of silica nanoparticles from Rice Husk Ash and its characterization. J. Sci. Ind. Res., 79(7), 656-660.

[9] Bai, H., Zhang, L., Gu, D., 2018, Micrometer-sized spherulites as building blocks for lotus leaf-like superhydrophobic coatings. Appl. Surf. Sci., 459, 54-62.

[10] Bardestani, R., Patience, G. S., Kaliaguine, S., 2019, Experimental methods in chemical engineering: specific surface area and pore size distribution measurements-BET, BJH, and DFT. Can. J. Chem. Eng., 97(11), 2781-2791.

[11] Bayer, I.S., 2020, Superhydrophobic coatings from ecofriendly

materials and processes: a review. Adv. Mater. Interfaces, 7(13), 2000095.

[12] Boukhelkhal, D., Guendouz, M., Bourdot, A., Cheriet, H., Messaoudi, K., 2021, Elaboration of bio-based building materials made from recycled olive core. MRS Energy Sustain., 8, 98-109.

[13] Cannio, M., Boccaccini, D. N., Caporali, S., Taurino, R., 2024, Superhydrophobic Materials from Waste: Innovative Approach. Clean Technol., 6(1), 299-321.

[14] Carlsen, M. M. H., Saito, Y., 2024, Phase diagram of SiO2 crystallization upon rice husk combustion to control silica ash quality. J. Waste Manag., 182, 55-62.

[15] Castillo, J., Galarza-Acosta, G. L., 2024, Superhydrophobic silica nanoparticles produced from rice husks, wettability at the macro-and nanoscale. Appl. Phys. A: Mater. Sci. Process, 130(2), 102.

[16] Chandrasekhar, S., Pramada, P.N., Praveen, L., 2005, Effect of organic acid treatment on the properties of rice husk silica. J. Mater. Sci. 40, 6535-6544.

[17] Chandrasekhar, S., Pramada, P. N., Majeed, J., 2006, Effect of calcination temperature and heating rate on the optical properties and reactivity of rice husk ash. J. Mater. Sci., 41, 7926-7933.

[18] Cho, Y. H., Jeong, S., Kim, S. J., Kim, Y., Lee, H. J., Lee, T. H., Park, H. B., Park, H., Nam, S. E., Park, Y. I., 2021, Sacrificial graphene oxide interlayer for highly permeable ceramic thin film composite membranes. J. Membr. Sci., 618, 118442.

[19] Danu, S., 2008, UV-curing of titanium dioxide pigmented epoxy acrylate coating on ceramic tiles. J. Ceram. Soc. Jpn., 116(1356), 896-903.

[20] Endale, S. A., Taffese, W. Z., Vo, D. H., Yehualaw, M. D., 2022, Rice husk ash in concrete. Sustainability, 15(1), 137.

[21] Fernandes, I. J., Santos, R. V., Santos, E. C. A. D., Rocha, T. L. A. C., Domingues Junior, N. S., Moraes, C. A. M., 2018, Replacement of commercial silica by rice husk ash in epoxy composites: a comparative analysis. Mat. Res., 21(3), e20160562.

[22] Gómez-García, R., Campos, D. A., Aguilar, C. N., Madureira, A. R., Pintado, M., 2021, Valorisation of food agro-industrial by-products: From the past to the present and perspectives. J. Environ. Manag., 299, 113571.

[23] Gomes, L. S., Furtado, A. C. R., Souza, M. C., 2018, Silica and its Peculiarities. Rev. Virtual Quim., 10(4), 1018-1038.

[24] Guendouz, M., Boukhelkhal, D., 2018, Physical and mechanical properties of cement mortar made with brick waste. In MATEC Web of Conferences (Vol. 149, p. 01077). EDP Sciences.

[25] Guendouz, M., Boukhelkhal, D., 2018, Properties of dune sand concrete containing coffee waste. In MATEC web of conferences (Vol. 149, p. 01039). EDP Sciences.

[26] Guendouz, M., Boukhelkhal, D., 2019, Properties of flowable sand concrete containing ceramic wastes. J. Adhes. Sci. Technol., 33(24), 2661-2683.

[27] Guendouz, M., Boukhelkhal, D., Bourdot, A., 2021, Recycling of floor tile waste as fine aggregate in flowable sand concrete. In Advances in Green Energies and Materials Technology: Selected Articles from the Algerian Symposium on Renewable Energy and Materials (ASREM-2020) (pp. 223-229). Springer Singapore.

[28] Guendouz, M., Boukhelkhal, D., Mechantel, A., Boukerma, T., 2023, Valorization of coffee waste as bio-aggregates in crushed sand concrete production. Environ. Eng. Manag. J., 22(1).

[29] Islam, M. T., Hossen, M. F., Asraf, M. A., Zakaria, C. M., 2024, Production and Characterization of Silica from Rice Husk: An Updated Review. Asian J. Chem. Sci., 14(2), 83-96.

[30] Iwuanyanwu, O., Gil-Ozoudeh, I., Okwandu, A. C., Ike, C. S., 2024, The role of green building materials in sustainable architecture: Innovations, challenges, and future trends. Int. J. Appl. Res. Soc. Sci., 6(8), 1935-1950.

[31] Jembere, A. L., Fanta, S. W., 2017, Studies on synthesizing silica powder from rice husk ash as reinforcement filler in rubber tire tread part: Replacement of commercial precipitated silica. Int. J. Mater. Sci. Appl., 6(1), 37-44.

[32] Junaidi, M. U. M., Haji Azaman, S. A., Ahmad, N. N. R., Leo, C. P., Lim, G. W., Chan, D. J. C., Yee, H. M., 2017, Superhydrophobic coating of silica with photoluminescence properties synthesized from rice husk ash. Prog. Org. Coat., 111, 29-37.

[33] Jyoti, A., Singh, R. K., Kumar, N., Aman, A. K., Kar, M., 2021, Synthesis and properties of amorphous nanosilica from rice husk and its composites. Mater. Sci. Eng. B, 263, 114871.

[34] Kumar, A., Negi, S., Kar, S., 2024, A study on functionalization process of silicon dioxide nanoparticles for hydrophobic coating applications. Surf. Interface and Anal., 56(7), 447-455.

[35] Kung, C. H., Sow, P. K., Zahiri, B., Mérida, W., 2019, Assessment and interpretation of surface wettability based on sessile droplet contact angle measurement: challenges and opportunities. Adv. Mater. Interfaces, 6(18), 1900839.

[36] Lejnieks, J., Mourran, A., Tillmann, W., Keul, H., Möller, M., 2010, Thin film of Poly (acrylic acid-co-allyl acrylate) as a Sacrificial Protective Layer for Hydrophilic Self Cleaning Glass. Materials, 3(5), 3369-3384.

[37] Li, D., Xu, F., 2020, The study of the possibility of silicon dioxide coatings modified by (3-aminopropyl) triethoxysilane as protective materials for stone. J. Coat. Technol. Res., 17(2), 563-572.

[38] Lima, S. P. B. D., Vasconcelos, R. P. D., Paiva, O. A., Cordeiro, G. C., Chaves, M. R. D. M., Toledo Filho, R. D., Fairbairn, E. D. M. R., 2011, Production of silica gel from residual rice husk ash. Quim. Nova, 34, 71-75.

[39] Liou, T. H., Yang, C. C., 2011, Synthesis and surface characteristics of nanosilica produced from alkali-extracted rice husk ash. Mater. Sci. Eng. B, 176(7), 521-529.

[40] Matinfar, M., Nychka, J. A., 2023, A review of sodium silicate solutions: Structure, gelation, and syneresis. Adv. Colloid. Interface Sci. 322, 103036.

[41] Moosa, A. A., Saddam, B. F., 2017, Synthesis and Characterization of Nanosilica from Rice Husk with Applications to Polymer Composites. Am. J. Mater. Sci., 7(6), 223-231.

[42] Nakano, K., Ito, T., Onouchi, Y., Yamanaka, M., Akita, S., 2016, Importance of gelation and crystallization for producing superhydrophobic surfaces from mixtures of hydrogenated castor oil and fatty acids. Colloid Polym. Sci., 294, 69-75.

[43] Nayak, P. P., Datta, A. K., 2021, Synthesis of SiO_2-nanoparticles from rice husk ash and its comparison with commercial amorphous silica through material characterization. Silicon, 13(4), 1209-1214.

[44] Nehan, P. Z. Z., Akbar, A. A., Karim, M. I. N., Fahriza, R. A., Zainuri, M., 2023, Synthesis of Silica from Rice Husk Waste for Hydrophobic Material as an Anti-Water Coating for Eyeglasses. J. Fis. dan Apl., 19(2), 44-48.

[45] Nzereogu, P. U., Omah, A. D., Ezema, F. I., Iwuoha, E. I., Nwanya, A. C., 2023, Silica extraction from rice husk: comprehensive review and applications. Hybrid Adv., 4, 100111.

[46] Prasad, R., Pandey, M., 2012, Rice husk ash as a renewable source for the production of value added silica gel and its application: an overview. Bull. Chem. React. Eng. Catal., 7(1), 1-25.

[47] Samy, A., Ismail, A. M., Ali, H., 2023, Environmentally friendly mesoporous SiO_2 with mixed fiber/particle morphology and large surface area for enhanced dye adsorption. J. Mater. Sci., 58(4), 1586-1607.

[48] Santos, T., Hennetier, L., Costa, V. A., Costa, L. C., 2020, Microwave vs conventional porcelain firing: macroscopic properties. Int. J. Appl. Ceram. Tec., 17(5), 2277-2285.

[49] Sarma, H. H. and Paul, A., 2024, Turning Waste into Wealth: Exploring Strategies for Effective Agricultural Waste Management. [Online]. Avaiable: https://vigyanvarta.in/Article Details.aspx?id=1980

[50] Sauthier, G., Segura, J. J., Fraxedas, J., Verdaguer, A., 2014, Hydrophobic coating of mica by stearic acid vapor deposition. Colloids Surf. A: Physicochem. Eng. Asp., 443, 331-337.

[51] Ugheoke, I. B., Mamat, O., 2012, A critical assessment and new research directions of rice husk silica processing methods and properties. Maejo Int. J. Sci. Technol., 6(03), 430-448.

[52] Varışli, S.Ö., Taşkıran, F., Öztürk, B., Çiçek, B., 2023, Effect of SiO2/Al2O3 ratio on the whiteness of ceramic tile engobes with low zircon content. Cerâmica, 69, 254-260.

[53] Vidal, L., Joussein, E., Colas, M., Cornette, J., Sanz, J., Sobrados, I., Gelet, J. L., Absi, J., Rossignol, S., 2016, Controlling the reactivity of silicate solutions: A FTIR, Raman, and NMR study. Colloids Surf. A: Physicochem. Eng. Asp., 503, 101-109.

[54] Wen, M., Zhong, J., Zhao, S., Bu, T., Guo, L., Ku, Z., Peng, Y., Huang, F., Cheng, Y.B., Zhang, Q., 2017, Robust transparent superamphiphobic coatings on non-fabric flat substrates with inorganic adhesive titania bonded silica. J. Mater. Chem. A, 5(18), 8352-8359.

[55] Wu, Y., Tan, X., Wang, Y., Tao, F., Yu, M., Chen, X., 2022, Nonfluorinated, transparent, and antireflective hydrophobic coating with self-cleaning function. Coll. Surf. A Colloid Surf. A Physiochem. Eng. Asp., 634, 127919.

[56] Yuan, S., Hou, Y., Liu, S., Ma, Y. A., 2024, Comparative Study on Rice Husk, as Agricultural Waste, in the Production of Silica Nanoparticles via Different Methods. Materials, 17(6), 1271.

[57] Yuvakkumar, R., Elango, V., Rajendran, V., Kannan, N., 2014, High-purity nanosilica powder from rice husk using a simple chemical method. J. Exp. Nanosci., 9(3), 272-281.

[58] Zou Y. and Yang T., Rice Husk, Rice Husk Ash and Their Applications. In: Cheong L-Z, Xu X (eds) Rice Bran and Rice Bran Oil, pp 207-246. AOCS Press, Champaign, 2019.

[59] Zulfiqar, U., Subhani, T., Husain, S. W., 2016, Synthesis of silica nanoparticles from sodium silicate under alkaline conditions. J. Sol-Gel Sci. Techn., 77, 753-758.